Max-Planck-Institut
für Mathematik
in den Naturwissenschaften
Leipzig

Hydration of ionic species studied by the reference interaction site model with a repulsive bridge correction

(revised version: February 2008)

by

Gennady Chuev, Maxim V. Fedorov, Sandro Chiodo, Nino Russo, and Emilia Sicilia

Preprint no.: 20 2008

Hydration of ionic species studied by the reference interaction site model with a repulsive bridge correction

Gennady N. Chuev[1], Maxim V. Fedorov[2,3],
Sandro Chiodo[4], Nino Russo[4], Emilia Sicilia[4]

[1] *Institute of Theoretical and Experimental Biophysics, Russian Academy of Sciences, Pushchino, Moscow Region, 142290, Russia*

[2] *Max Planck Institute for Mathematics in the Sciences, Inselstrasse 22, Leipzig, 04103, Germany*

[3] *Department of Chemistry, University of Cambridge, Lensfield Road, Cambridge, CB2 1EW, UK and*

[4] *Dipartimento di Chimica and Centro di Calcolo ad Alte Prestazioni per Elaborazioni Parallele e Distribuite-Centro d'Eccellenza MIUR, Universitá della Calabria, I-87030 Arcavacata di Rende (CS), Italy*

We have tested the reference interaction site model (RISM) for the case of the hypernetted chain (HNC) and the partially linearized hypernetted chain (PLHNC) closures improved by a repulsive bridge correction (RBC) for ionic hydrated species. We have analyzed the efficiency of the RISM/HNC+RBC and RISM/PLHNC+RBC techniques for decomposition of the electrostatic and the nonpolar hydration energies on the energetic and the enthalpic parts for polyatomic ions when the repulsive bridge correction is treated as a thermodynamic perturbation, and investigate the repulsive bridge effect on the electrostatic potential induced by solvent on solute atoms. For a number of univalent and bivalent atomic ions, molecular cations and anions the method provides hydration energies deviating only by several percents from the experimental data. In most cases the enthalpic contributions to the free energies are also close to the experimental results. The above models are able to satisfactory predict the hydration energies as well as the electrostatic potential around the ionic species. For univalent atomic ions they also provide qualitative estimates of the Samoilov activation energies.

Introduction

Ion hydration is one of the most fundamental physico-chemical processes occurring in chemical and biological systems. Many efforts have been spent for theoretical and experimental studies of ion hydration properties[1–4] and various theoretical methods have been developed to investigate solvation effects. The dielectric continuum model[5] treats solvent molecules in an implicit way, while molecular simulations[6,7] and methods based on the integral equation theory (IET)[8–32] are considered as explicit solvation models. Although the molecular simulations are more realistic and give the most reliable insight into microscopic processes, they dramatically increase the computational time required for the calculations. The IET provides an alternative 'low-cost' technique for treating molecular effects in liquids[8–32]. At present there are several approaches based on integral equations. The molecular Ornstein–Zernike (MOZ) theory is the method to calculate three- dimensional (3D) solvation structure in molecular liquids. The MOZ theory treats the orientation dependence of intermolecular interactions through the rotational invariant expansions of interaction potentials and correlation functions[9]. The recent MOZ calculations[10–14] have indicated that the theory is able to reproduce the thermodynamic, dielectric, and structural properties for aprotic solvents. Another method is the reference interaction site model (RISM) pioneered by Chandler and Andersen[8] and then extended to the polar liquids by the XRISM treatment[17,18]. The theory is based on calculations of radial distribution functions (RDF) via the site-site Ornstein-Zernike (SSOZ) integral equation. The theory has been successfully applied to calculate structural and thermodynamic properties of various chemical and biological systems[16,19]. Recently, 3D extensions of the RISM theory have been developed to obtain 3D correlation functions of interaction sites of solvent molecules around a solute of arbitrary shape[20–31,34,35].

In the original XRISM procedure[17,18] the hypernetted chain closure (HNC) was employed to take into acount the nonlinear response of solvent. The advantage of the RISM/HNC approximation resides in the fact it is well suited for the description of liquids containing polar solutes. However, the predictions coming from this method are rather poor for the thermodynamics of hydrophobic solvation and provide only a qualitative picture for the solvation of charged solutes, since the RDF amplitudes responsible for hydrogen bonding are overestimated. Although the 1D HNC closure provides physically reasonable

results for polar polyatomic solutes hydrated in water at normal conditions, it can become divergent in the case of a very deep well of the attractive potential between the solute and individual solvent sites. To eliminate this artefact, a partial linearization of the HNC closure (PLHNC) have been proposed in Refs.[26,27]. In fact, it combines the HNC for the region of the density profile depletion and the mean spherical approximation for the regions of enrichment.

Beyond the RISM/HNC and RISM/PLNHC approximations, an additional effective repulsion has to be introduced to account solute steric constrains. The orientational average of the Boltzmann factor for a repulsive core potential of the whole solvent molecule has been incorporated in the 3D RISM/HNC closure[22] to account the steric constrains. Kovalenko and Hirata[29] have extended this repulsive bridge correction (RBC) to the one-dimensional RISM approach. Since it operates only with the solute-solvent RDFs, it is essentially simpler and faster than the 3D RISM treatment. On the other hand, the predictive capabilities of the 1D RISM/HNC improved by the RBC are comparable with that obtained by the sophisticated 3D RISM treatment[33].

Due to the simplicity and the accuracy of the method, the RISM/HNC model improved by the RBC (RISM/HNC+RBC) is a promising method to study complex solutions including polyatomic ions. In general, accurate calculations of solvated molecules have to take into account of quantum degrees of freedom[36]. For this purpose, a combined RISM - self-consistent-field (SCF) approach has been developed more than a decade ago[37–39]. In this method the solvent structure is treated on the classical footing with use of the RISM theory, while the electronic structure of the solute is calculated by quantum chemistry methods at various level of accuracy. Apart of the original RISM-SCF formulations[37–39], there are some more sophisticated models based on this approach which take into account 3D details of the solvent structure[40,41] and the electron density distribution[42] as well as alternative couplings for the solute-solvent interactions[43]. However, for the purposes of our study we decided to employ the simplest estimates and apply the quantum chemical calculations only to evaluate changes in the electronic energy of the solute.

The goal of our study is to apply the RISM/HNC+RBC and the RISM/PLHNC+RBC for investigations of thermodynamic and structural properties of hydrated atomic and molecular ions. We will focus on the effect of the repulsive bridge corrections on the calculated values of the free energy of the charged molecular solutes. Among other quantities we will evaluate

the Samoilov activation energy (amount of energy required to strip a water molecule away from the first solvation shell of an ion as compared to that for another water molecule) and will compare the results with the Samoilov experiments on viscosity[44]. We will calculate the RDFs and the electrostatic potential around different ions and compare them with results of molecular dynamics (MD) simulations. The calculated thermodynamic parameters of ionic hydration will be also compared with available experimental data. In addition, we will analyze the efficiency of the RISM/HNC+RBC and RISM/PLHNC+RBC technique for decomposition of the electrostatic and the nonpolar hydration energies on the entropic and the enthalpic parts for polyatomic ions when the repulsive bridge correction is treated as thermodynamic perturbation. We will also investigate the repulsive bridge effect on the electrostatic potential induced by the solvent on solute atoms.

We will outline the method in Section II, the details of calculations will be described in Section III, while the results of the calculations will be presented and discussed in Section IV.

Method

Following Refs.[37–39] the solvation energy (ΔG) of a hydrated molecule can be defined as the sum of the change in the intramolecular energy of solute (ΔE) and the solvation free energy ($\Delta\mu$) which contains all of the contributions from the solvent:

$$\Delta G = \Delta E + \Delta\mu. \tag{1}$$

The change in the intramolecular energy ΔE is due to the polarization of the solute electron density interacting with the solvent. To estimate this quantity we employ the linear response theory (LRT)[45] which gives us the following equation:

$$\Delta E = \frac{1}{2}\sum_u V_u \Delta q_u, \tag{2}$$

where Δq_u is the change in partial charge of the u-site, which is determined as the difference between the partial charges of the solute in vacuum and solvent, respectively, while V_u is the electrostatic potential induced by the solvent at the solute u-site. In the case of the water solvent it can be expressed via total solute-oxygen (h_{uO}) and solute-hydrogen (h_{uH}) correlation functions

$$V_u = 4\pi n_0 \int_0^\infty [2q_H h_{uH}(r) + q_O h_{uO}(r)] r dr, \tag{3}$$

where n_0 is the averaged water density, while q_H and q_O are hydrogen and oxygen charges of water molecule. We calculate the correlation functions by the RISM equation:

$$\mathbf{H}^{uv} = \mathbf{W}^u * \mathbf{C}^{uv} * [\mathbf{W}^v + n_0\mathbf{H}^{vv}]. \tag{4}$$

The superscripts v and u refer to the solvent and the solute, respectively, the symbol $*$ corresponds to the convolution integration, the matrix elements of $\mathbf{H}$ and $\mathbf{C}$ are matrices built from the site-site total and the direct correlation functions, respectively, and $\mathbf{W}$ is the intramolecular correlation matrix. The Fourier transform of the matrix elements of $\mathbf{W}$ is given by $\widehat{w}_{ij}(k) = \delta_{ij} + (1-\delta_{ij})\sin(kl_{ij})/kl_{ij}$, where i and j denote molecular sites of the same molecule, and l_{ij} is the intramolecular distance between i and j sites. In the above equation, the solvent matrices $\mathbf{W}^v$ and $\mathbf{H}^{vv}$ do not change during the calculations and we regard them as input data. They are calculated separately and stored in computer memory. Both the matrices $\mathbf{H}$ and $\mathbf{C}$ can be obtained by Eqn. (4) coupled with a closure relation:

$$c_{uj}(r) = \exp[-\beta U_{uj}(r) + \gamma_{uj}(r) + B_{uj}(r)] - \gamma_{uj}(r) - 1, \quad j = O, H, \tag{5}$$

here $U_{uj}(r)$ is the intermolecular site-site potential, $\gamma_{uj}(r) = h_{uj}(r) - c_{uj}(r)$ is the indirect correlation function, $B_{uj}(r)$ is a bridge function, $\beta = (k_B T)^{-1}$ where k_B is the Boltzmann constant, and T is the absolute temperature. The case $B = 0$ corresponds to the HNC closure. The PLHNC[26,27] applies linearization of the exponent in (5) depending on the sign of the index $I_{uj}(r) = -\beta U_{uj}(r) + \gamma_{uj}(r) + B_{uj}(r)$:

$$c_{uj}(r) = \exp[I_{uj}(r)] - \gamma_{uj}(r) - 1, \quad I_{uj}(r) < 0, \quad c_{uj}(r) = -\beta U_{uj}(r) \quad I_{uj}(r) > 0. \tag{6}$$

The solute-solvent intermolecular potentials are represented by the Lennard-Jones (LJ) and the coulomb terms:

$$U_{uj}(r) = 4\varepsilon_{uj}([\frac{\sigma_{uj}}{r}]^{12} - [\frac{\sigma_{uj}}{r}]^{6}) + \frac{q_u q_j}{r}. \tag{7}$$

The LJ parameters σ_{uj} and ε_{uj} are determined according to the standard combining rules, $\sigma_{uj} = (\sigma_u + \sigma_j)/2$ and $\varepsilon_{uj} = \sqrt{\varepsilon_u \varepsilon_j}$.

To complete the expression for the hydration energy (1) we should derive the expression for the excess chemical potential $\Delta\mu$ via correlation functions. In the case of HNC approximation there is an explicit formula for $\Delta\mu$[46]:

$$\beta\Delta\mu = -4\pi n_0 \sum_{uj} \int_0^\infty [c_{uj}(r) + \frac{1}{2} c_{uj}(r) h_{uj}(r) - \frac{1}{2} h_{uj}^2(r)] r^2 dr, \tag{8}$$

while for the PLHNC it is expressed as[26]

$$\beta\Delta\mu_{PLHNC} = -4\pi n_0 \sum_{uj} \int_0^\infty [c_{uj}(r) + \frac{1}{2}c_{uj}(r)h_{uj}(r) - \frac{1}{2}h_{uj}^2(r)\Theta(-h_{uj}(r))]r^2 dr. \quad (9)$$

The Kirkwood charging formula[47] can be employed in the general case, it is written in the site-site formalism as:

$$\Delta\mu = 4\pi n_0 \sum_{uj} \int_0^1 d\lambda \int_0^\infty [1 + h_{uj}(r,\lambda)] \frac{\partial U_{uj}(r,\lambda)}{\partial\lambda} r^2 dr, \quad (10)$$

where λ is the coupling parameter. This relation requires calculation of solute-solvent correlation functions $h_{uj}(r,\lambda)$ at different values of λ. Typically, two coupling parameters λ_{nel} and λ_{el} are introduced to calculate the nonpolar and the electrostatic free energy contributions, respectively[28]. The former is considered as a scaling factor of the LJ radius, i.e. $\sigma_{uj}(\lambda_{nel}) = \lambda_{nel}\sigma_{uj}$, while the coupling parameter λ_{el} is introduced as a scaling factor of the solute charge, $q_u(\lambda_{el}) = \lambda_{el}q_{uj}$. Thus, we express $\Delta\mu$ as

$$\Delta\mu = \Delta\mu_{nel} + \Delta\mu_{el}, \qquad \Delta\mu_{el} = \sum_u q_u \int_0^1 V_u(\lambda_{el}q_u)d\lambda_{el}.$$

Using linear approximation for integration over λ_{el}, we rewrite it as

$$\Delta\mu_{el} \approx \sum_{su} q_u[V_u(0) + \frac{q_s}{2}V'_{su}], \quad (11)$$

where V'_{su} is the matrix of the approximating coefficients, while $V_u(0) = V_u(q_u = 0)$ is the nonzero potential arising even for nonpolar solute due to different distribution of oxygen and hydrogen sites of water molecules around the solute. It is responsible for asymmetry of solvation of cations and anions[48,49]. If the matrix $V'_{su} = \partial V_s/\partial q_u$ is charge independent, we have quadratic dependence of the solvation energy on the solute charge, which corresponds to the LRT approach. In general case, the dependence $V'_{su}(\lambda_{el})$ is smooth and can be estimated with the use of few intermediate points of integration.

To reduce the overestimated hydrogen bonding in the RISM/HNC(PLHNC) models we use the repulsive bridge correction (RBC)[29] in the corresponding closures:

$$\exp[-B_{ij}(r)] = \prod_{l\neq j} w_{il}(r) * \exp[-4\beta\epsilon_{lj}(\frac{\sigma_{lj}}{r})^{12}]. \quad (12)$$

Such correction factor has been proposed for the 3D orientational reduction of the MOZ equation for an one-component molecular liquid[22]. Similar empirical bridge corrections have

been also employed to treat hydration of organic molecules by the 3D RISM scheme[28] as well as to evaluate electronic structure of organic solutes by the combined 3D RISM/QM method[50]. Kovalenko and Hirata[29] proposed to take the repulsive core as the sum of the LJ terms, since the orientational average of the potential yields a soft repulsion extending beyond the LJ repulsive core throughout the first hydration shell and provides the correct dependence of the hydration chemical potential on the solute size[29].

The nonelectrostatic contribution $\Delta\mu_{nel}$ is calculated by the perturbation scheme proposed in Ref.[29]:

$$\beta\Delta\mu_{nel} = \beta\Delta\mu_{nel}^{HNC} + 4\pi n_0 \sum_{uj} \int_0^\infty g_{uj}^{HNC}(r)[\exp[-B_{uj}(r)] - 1]r^2 dr, \tag{13}$$

where the correlation functions are taken at zero bridge function $B_{uj}(r) = 0$, and $\Delta\mu_{nel}^{HNC}$ is calculated by (8). The perturbation treatment is essentially simpler and faster than the complete thermodynamic integration, but provides reasonable accuracy for evaluations of hydrated hydrophobic and polar organic solutes[29,51].

To describe the solvation properties we decompose the excess chemical potential into the enthalpic and the entropic contributions. Since experiments are most commonly done at fixed pressure p, it is convenient to decompose the hydration chemical potential into the excess solvation entropy ΔS and the excess solvation enthalpy ΔH in the following manner:

$$\Delta S = \left(\frac{\partial\Delta\mu_{ex}}{\partial T}\right)_p, \quad \Delta E_s = \Delta\mu + T\Delta S. \tag{14}$$

But this definition demands calculations of the solvent RDFs on each step of the temperature increase. Another way to calculate these contributions is to express the excess chemical potential as a sum of an energetic term and an entropic one which are both functions of only the solute-solvent interactions:

$$\Delta E_{solv} = n_0 \sum_{uj} \int g_{uj}(r)U_{uj}(r)d\mathbf{r}, \quad T\Delta S_u = \Delta E_{solv} - \Delta\mu. \tag{15}$$

In the case one does not need to calculate the derivative $\partial\Delta\mu/\partial T$ and, therefore, the integral (15) can be easily evaluated. The difference $\Delta E_s - \Delta E_{solv}$ is the reorganization energy of the solvent, which does not contribute to the chemical potential since it is exactly counterbalanced by a term in the solvation entropy.

Computational details

We have tested our approach for different atomic and molecular ions. The LJ parameters of the ions have been derived from the OPLS force field[52,53], they are listed in Table 1 where we have used the notations similar to that in Ref.[53]. The small Lennard-Jones parameter $\sigma_H = 0.4$Å is attributed to the highly charged hydrogen sites in order to avoid numerical singularities. Although the OPLS force field require the geometric combination rule for the LJ solute-solvent parameters, we have employed the arithmetic rules described above, because the geometric rule results in the small size of hydrogen and hence to abnormal hydrogen bonding.

Since the hydration of ionic species depends significantly on the values of partial charges of solute atoms, we have derived the solute charges using QM calculations instead of direct use of the OPLS charges for the relevant molecular ions. To derive the partial atomic charges of the solutes we have implemented the Kollman procedure[54] with the deMon program based on the linear combination of Gaussian-type orbitals[55]. This method is able to evaluate the charges by fitting the electrostatic potential (ESP). The ESP procedure leads to the following expression of the electronic charges[38]:

$$q_i^{(e)} = -\sum_j D_{ij} tr(\mathbf{PA})_j - \xi \sum_j D_{ij}, \tag{16}$$

where the matrix $\mathbf{D}$ is equal to inverse matrix $[\sum_l \omega_l / \delta r_{lj} \delta r_{lj}]^{-1}$, where $\delta r_{li} = |\mathbf{r}_l - \mathbf{r}_i|$ is the distance between the grid point l and the solute atom i, while ω_l is its weight, $\mathbf{P}$ is the self-consistent density matrix and $\mathbf{A}$ is the supermatrix whose elements are:

$$A_{\mu\nu i}(\mathbf{r}) = \sum_l \frac{\omega_l}{\delta r_{li}} \langle \phi_\mu | \frac{1}{|\mathbf{r} - \mathbf{r}_l|} | \phi_\nu \rangle, \tag{17}$$

where ϕ_ν are the contracted cartesian gaussian functions. The Lagrange multiplier ξ can be expressed as:

$$\xi = \frac{-\sum_{ij} D_{ij} tr(\mathbf{PA})_j - N_e}{\sum_{ij} D_{ij}}, \tag{18}$$

where N_e is the total number of the electrons. The extra grid points inside the 1.4 van-der-Waals radius were removed to avoid ESP singularities near to the nuclear position of the solute. We excluded also the grid points outside the 2.0 van-der-Waals radius because the ESP integration over them do not influence numerically the charge values. The ESP calculations were carried out using a fixed Lebedev grid of 200 radial shell points and 1202 angular

points for each shell. All calculations have been performed at local density approximation (LDA) level using the exchange correlation functional derived by Vosko, Wilk, and Nusair[56] and double zeta for valence electrons plus one polarized function (DZVP)[58] as basis set. To avoid calculations of the four-center coulomb integrals, gaussian-type auxiliary A2 functions have been used. The numerical calculation of the density was performed employing directly the DZVP basis set for the numerical integration of the exchange correlation functional.

Although the self-consistent reaction field (SCRF) procedure can be adopted to evaluate the solvent-field solute charge polarization, the earlier estimates[45] have indicated the contribution of the polarization energy to the hydration free energy to be small for the considered charged species, therefore one can apply less sophisticated procedure to evaluate this contribution. In this work we have used more simplified LRT version and applied the Polarizable Continuum Model (PCM) to estimate the polarization contribution. Comparison of the PCM and the RISM-SCF evaluations[57] have indicated that both the methods predict similar mean force potentials, but there is a difference in the calculated polarization energies. Some advanced models[42] could be more accurate for evaluating partial changes, but, as a whole, the influence of the procedure evaluating partial charges on the free energy of the studied charges species is to be minor (see the next section).

Table 1 reports the difference between the solute gas-phase charges and the solute SCRF charges calculated by the Kollman method[54]. Although the deviation of the calculated charges from that parameterized by the OPLS[53] is about 10-15% it essentially affects the polarization energy ΔE of solutes.

The ESP charges were used as input data for RISM calculations. We employed the modified version of the extended simple point charge model for water[59]. The water density n_0 is assumed to be equal to 0.997 g/cm^3 at room temperature. For calculation of water RDFs we used a reformulation of the RISM with dielectric corrections[60,61]. For accurate screening of the long-range interactions within the framework of this method, the intermolecular Coulomb potential $q_i q_j / r$ is rescaled as $A(\epsilon) q_i q_j / r$ where the scalar factor A is defined via the phenomenological dielectric constant ϵ and the dipole moment m of the water molecule as

$$A = \frac{1 + \epsilon\,(3y - 1)}{3y\,(\epsilon - 1)}, \quad y = \frac{4\pi\beta\rho m^2}{9}. \tag{19}$$

We notice that this procedure is only applied for the solvent-solvent interaction potential, the solute-solvent Coulomb potential remains unchanged. This approach makes use of the

solute	site	σ(Å)	$\epsilon(\frac{kcal}{mol})$	q	Δq	solute	site	σ(Å)	$\epsilon(\frac{kcal}{mol})$	q	Δq
H_3O^+	HW	0.4	0.046	+0.5189	+0.025	OH^-	HW	0.4	0.046	+0.2463	-0.095
	OW	3.166	0.1554	-0.5569	-0.076		OW	3.166	0.1554	-1.2463	+0.071
NH_4^+	H	1.2	0.0157	+0.4683	-0.009	NH_2^-	H	1.2	0.0157	+0.2021	+0.087
	N3	3.25	0.17	-0.8732	+0.038		N3	3.25	0.17	-1.4042	-0.173
CN^-	C	3.816	0.086	-0.5693	+0.066	OCl^-	OW	3.166	0.1554	-0.6898	-0.077
	N3	3.25	0.17	-0.4307	-0.066		Cl	4.417	0.1178	-0.3102	+0.077
HO_2^-	HW	0.4	0.046	+0.3324	+0.071	HCC^-	CT	3.816	0.086	-0.1479	0.058
	OW	3.166	0.1554	-0.7572	-0.015		CT	3.816	0.086	-0.8521	-0.115
	OW	3.166	0.1554	-0.5752	-0.056		HC	2.5	0.03	0.0782	0.057
CH_3O^-	CT	4.2	0.3	+0.2024	-0.045	$CHOO^-$	C	3.816	0.086	+0.6228	+0.005
	O	3.15	0.25	-0.9785	-0.102		O2	2.96	0.21	-0.7367	-0.039
	HC	2.5	0.03	-0.0741	0.049		HC	2.5	0.03	-0.1494	+0.071
$(CH_3)_3C^+$	C+	3.55	0.07	+0.5588	+0.085	CH_3S^-	S	4.25	0.5	-0.9352	-0.108
	CT	3.5	0.066	-0.5352	-0.034		CT	4.2	0.3	-0.2767	+0.022
	HC	2.5	0.03	+0.222	+0.002		HC	2.5	0.03	+0.0707	+0.029
CH_3COO^-	C	3.75	0.105	+0.8061	-0.009	$CH_3NH_3^-$	N3	3.25	0.17	-0.3363	+0.107
	O2	2.96	0.21	-0.7809	-0.048		HC	2.5	0.03	+0.3456	-0.013
	CT	3.5	0.066	-0.4200	-0.033		CT	3.5	0.066	-0.1529	-0.032
	HC	2.5	0.03	+0.0569	+0.046		HC	2.5	0.03	+0.1508	-0.012

TABLE I: LJ parameters and atomic charges for molecular ions.

known asymptotic form of the correlation functions and, in general, more sophisticated nontrivial closures can be applied[62].

The solute-solvent correlation functions for pure water have been calculated by the wavelet-based algorithm[63–65] before fitting the charges and calculations of solute-solvent correlation functions. The method proposes an expansion of site-site correlation functions into the wavelet series and further calculations of the approximating coefficients. To solve the integral equations we have applied the hybrid scheme in which the coarse part of the

solution is calculated by wavelets with the use of the Newton-Raphson (NR) procedure, while the fine part is evaluated by the direct iterations. The Coifman 2 basis set is employed for the wavelet treatment of the coarse solution. We generated wavelets with $n = 4096$ grid points and $\delta r = 0.02645$Å step size, the number of approximating coefficients s_{max} is equal to 25 for each site-site correlation function, while the level of resolution is $j_0 = 4$. As well as in the conventional scheme, to speed up convergence we have initially solved RISM equations for uncharged solute species and then we have repeated the same calculations by increasing the charge using the previous solution as an initial guess. The system was gradually charged up to the target charge. The set is solved iteratively until the required accuracy is achieved. The precision parameter determining the measure of the accuracy is the root mean square residual equal to 10^{-6} for the NR loop and to 10^{-5} for the Picard iterations[63,65]. The electrostatic contribution $\Delta\mu_{el}$ to the free energy is calculated with the use of the charging procedure at five different values of coupling parameter λ_{el}.

Results and discussion

Earlier we have calculated the hydration free energies of atomic and molecular ions by the RISM/HNC within the OPLS force field[66,67], and indicated that the RISM/HNC model overestimates systematically the absolute values of hydration free energy for anions, and underestimates that for cations by 20-40%. Moreover the RISM/HNC procedure is not convergent in several cases. All these effects are due to overestimation of RDF amplitudes responsible for hydrogen bonding. The discrepancy becomes to be more pronounced for small sized solutes where hydrogen bonding effect is stronger. In this paper we have calculated the hydration energy for the series of atomic and molecular ions by the HNC+RBC and PLHNC+RBC models and decomposed the hydration energies into the enthalpic and entropic parts. Table 2 lists the calculated hydration energies, the enthalpies, and the entropies for atomic ions and the corresponding experimental data[45,68]. There is a difference between the enthalpic and energetic parts due to the difference in the entropic changes at constant pressure and volume, i.e. $\Delta\Delta H = \Delta H - \Delta E_s = T\alpha n_0(\partial\Delta\mu/\partial n_0)_T$, where α is the isobaric thermal expansion coefficient of pure water. Since the difference is small under normal conditions (several kcal/mol) and comparable with the accuracy of our calculations, we ignore it to simplify the evaluations of the enthalpic changes. As it is seen, the models

underestimate absolute values of the hydration energy for atomic ions. The predictive capabilities of the method decrease for very small and very large ionic solutes. The average error does not exceed 6% however the discrepancy becomes up to 20% in the case of Cs^+. The calculated electrostatic contribution to the hydration entropy is an good agreement with the experimental data, however the calculated total entropies deviate sufficiently from the experiment. This artefact is supposed to be mainly caused by inaccurate evaluations of the entropic part of nonelectrostatic contribution $\Delta\mu_{nl}$. The agreement between the calculated and experimental results is better for cations then that for anions due to minor effect of hydrogen bonding in the first case. Although the RISM/HNC+RBC provides less deviation from the experiment than that obtained by the RISM/PLHNC+RBC model, the difference between these two models is insignificant.

Ion	$-\Delta G$			$-\Delta H$			$-T\Delta S$		
	HNC	PLHNC	Exp	HNC	PLHNC	Exp	HNC	PLHNC	Exp
Li^+	107.3(-0.6)	105.5(-1.1)	122.1	112.4(-0.4)	109.6(-0.5)	130.9	5.0(0.2)	4.1(0.6)	8.8
Na^+	89.9(-2.7)	89.2(-3.3)	94.8	93.9(-1.3)	92.6(-1.5)	105.0	4.0(1.3)	3.5(1.8)	6.6
K^+	76.2(-6.2)	75.9(-6.9)	80.6	79.2(-2.8)	78.7(-3.1)	84.5	3.0(3.5)	2.8(3.8)	3.9
Rb^+	71.6(-8.2)	71.4(-8.9)	75.5	74.3(-3.5)	73.9(-3.9)	78.8	2.7(4.7)	2.5(5.1)	3.3
Cs^+	65.2(-12.1)	65.2(-12.9)	67.8	67.4(-4.8)	67.3(-5.3)	70.7	2.2(7.2)	2.1(7.6)	2.9
Mg^{2+}	426.4(2.4)	418.3(1.5)	454.2	430.3(2.2)	430.3(2.4)	476.4	29.0(-0.2)	12.0(0.9)	22.2
Ca^{2+}	364.6(1.2)	357.6(0.1)	379.5	368.1(1.9)	368.1(1.9)	396.1	12.6(0.8)	10.5(1.8)	16.6
Sr^{2+}	333.2(-1.6)	329.2(-2.6)	339.7	339.4(0.4)	339.4(0.2)	355.6	12.0(2.0)	10.1(2.8)	15.9
Ba^{2+}	304.9(-4.1)	302.4(-5.2)	314.0	311.6(-0.6)	311.6(-1.0)	327.2	10.6(3.5)	9.2(4.2)	13.2
F^-	117.9(1.9)	116.4(0.5)	107.0	124.7(3.3)	124.7(3.3)	115.4	9.9(1.4)	8.3(2.8)	8.4
Cl^-	81.3(-5.5)	81.1(-6.9)	78.1	84.0(0.5)	84.0(0)	82.1	2.9(6.0)	2.9(6.9)	4.0
Br^-	79.0(-6.7)	78.9(-8.0)	69.2	81.5(0)	81.5(-0.5)	72.1	2.6(6.7)	2.6(7.5)	2.9
I^-	69.3(-10.8)	69.2(-12.2)	60.3	70.6(-0.7)	70.6(-1.3)	61.5	1.4(10.1)	1.4(10.9)	1.2

TABLE II: The experimental[45,68] hydration energies and the electrostatic and nonelectrostatic contributions (in parenthesis) to the total excess chemical potential, the enthalpies, and the entropies for hydrated atomic ions (kcal/mol), calculated by the PLHNC+RBC and the HNC+RBC models.

To reveal structural properties of the atomic ions, we follow the idea of Hirata and

ion	Mg^{2+}	Ca^{2+}	Li^{+}	Na^{+}	K^{+}	Cs^{+}	Cl^{-}	Br^{-}	I^{-}
PLHNC+RBC	3.7	2.4	1.3	0.65	0.1	-0.21	-0.23	-0.28	-0.61
Exp[44]	2.61	0.45	0.73	0.25	-0.25	-0.33	-0.27	-0.29	-0.32

TABLE III: The calculated (PLHNC+RBC) and the experimental activation energies (kcal/mol) for various hydrated ions.

Chong[69] and calculate the activation energy required to strip a water molecule away from the first solvation shell of an atomic ion as compared to that for another water molecule to its next coordination shell. For this purpose we use the following method which is similar to that has been used in Refs.[69,70] – we evaluate the site-site mean force potentials $w_{uj} = -\beta^{-1}\ln(g_{uj}(r))$, where $g_{uj}(r)$ is the ion-oxygen and ion-hydrogen RDFs for cations and anions, respectively. Then we evaluate the activation energy E_i as a difference between the first maximum and the first minimum of the corresponding mean force potential (mfp). Finally, the relative activation energy ΔE of a water molecule in an ion coordination shell is calculated as $\Delta E = E_i - E_0$, where E_0 is the activation energy of a water molecule transferring from a first shell around another water molecule to its next coordination shell, which is evaluated via the corresponding hydrogen-oxygen mfp of pure water. Table 3 lists the results calculated by the PLHNC+RBC model and the Samoilov data on the activation energies extracted from the viscosity experiments[44] for various hydrated ions. As it is seen, there is qualitative agreement between the experimental and the calculated data for monovalent ions. The theory overestimates the activation energies by 0.4 kcal/mol for atomic cations and provides quite accurate results for anions. But the theory fails for bivalent ions. The latter may be caused by many-body effects of hydrogen bonding formation, which can not be interpreted in terms of site-site mpf, but requires 3D evaluations.

We have also calculated the hydration energies, the enthalpies, and the entropies for polyatomic ions. Table 4 lists the experimental results[45,68] and data calculated by the PLHNC+RBC and HNC+RBC models. Although the theory overestimates the absolute values of hydration energy for polyatomic cations and underestimates for polyatomic anions, the average deviation does not exceed 6%. The difference between the calculated and experimental hydrations energies increases for very small and very large ionic solutes like as for atomic ions. The evaluations of the entropic contributions are less satisfactory

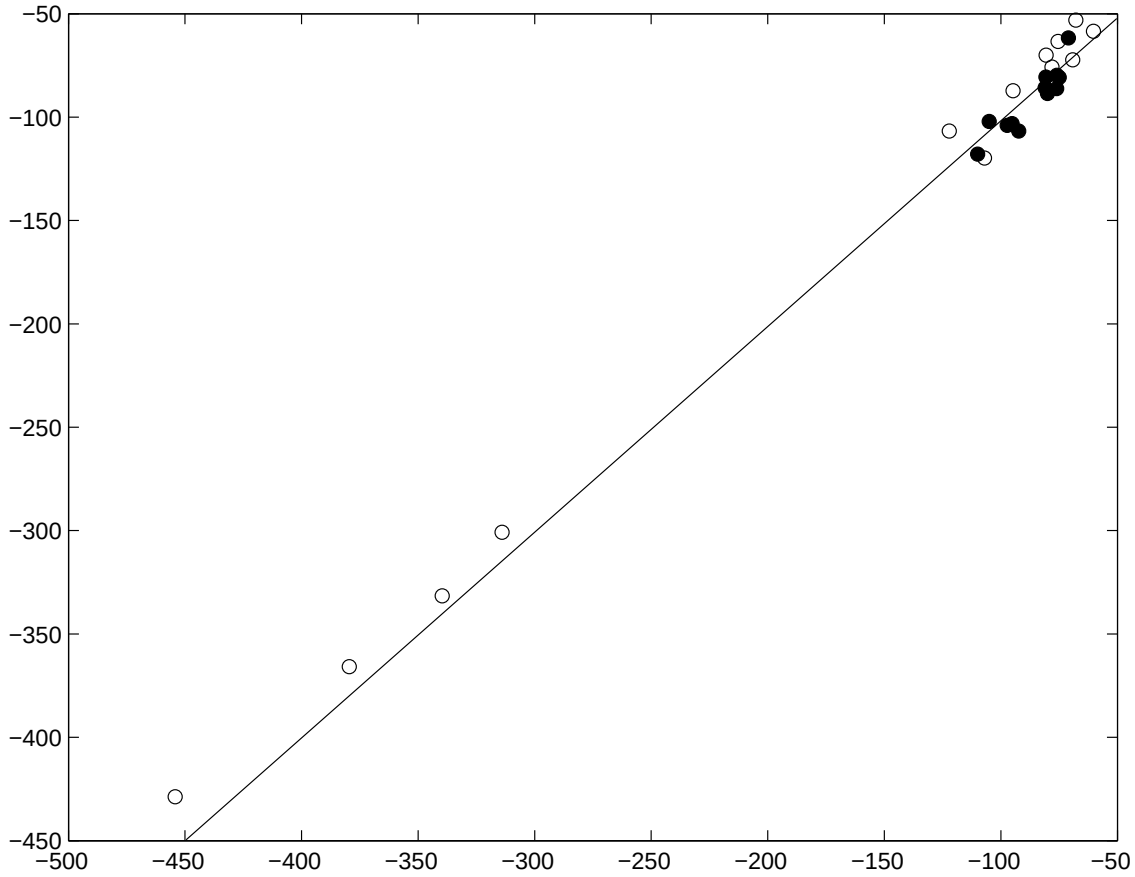

FIG. 1: The computed (RISM/PLHNC+RBC) versus the experimental[45,68] hydration free energies for (in kcal/mol) for molecular and atomic ions. The atomic ions are indicated by open circles, while the polyatomic ones by filled circles.

for both the HNC+RBC and the PLHNC+RBC models. The influence of intramolecular solute contribution ΔE and nonlectrostatic contribution $\Delta\mu_{nl}$ are small with respect to the electrostatic one $\Delta\mu_{el}$. Such behavior is typical for ionic systems and has been reported before[45]. Table 5 proves this effect, indicating the electrostatic (S_{el}), the nonelectrostatic (S_{nel}), and the polarization (S_{pol}) contributions to the entropies of hydrated ions (kcal/mol). As it is seen, the nonpolar contribution is overestimated. By our opinion this artefact is caused by that the thermodynamic perturbation theory is not appropriate for estimations in this case, since the main contribution is determined by the cavity effect. In principle, the later may be eliminated by an appropriate choice of the bridge for the nonelectrostatic part[73], but the study of this effect is beyond the scope of this paper. Figure 1 and Figure 2

Ion	$-\Delta G$			$-\Delta H$		
	HNC	PLHNC	EXP	HNC	PLHNC	EXP
OH^-	119.5(-1.6)	118.3(-2.9)	110.0	135.2(0.8)	129.4(0.5)	120.1
CN^-	81.6(-0.8)	81.6(-2.1)	75.0	85.5(2.3)	85.4(2.1)	79.4
OCl^-	83.8(-3.2)	83.6(-4.5)	80.7	90.9(2.4)	90.5(2.1)	
NH_4^+	86.8(-1.0)	84.0(-2.5)	81.0	91.6(0.9)	87.7(0.4)	87.6
$HCOO^-$	84.1(2.8)	84.4(1.3)	80.0	89.8(4.9)	89.7(4.8)	85.9
CH_3O^-	99.2(3.9)	98.9(2.5)	95.2	101.2(6.6)	101.4(6.4)	
HCC^-	87.7(-1.5)	87.6(-2.8)	76.1	95.0(2.1)	94.7(1.9)	
NH_2^-	108.7(-2.0)	108.2(-3.5)	92.3	119.7(1.1)	118.5(0.7)	
HO_2^-	103.5(0.5)	103.(-0.7)	97.3	113.8(2.6)	112.7(2.5)	
H_3O^+	103.1(-1.0)	99.5(-2.5)	105.0	107.7(0.8)	104.5(0.4)	113.9
CH_3COO^-	86.6(2.0)	87.9(0.8)	80.0	94.0(6.0)	95.0(5.9)	
$(CH_3)_3C^+$	57.8(-0.3)	59.1(-1.8)		57.9(5.4)	58.3(5.4)	
CH_3S^-	75.2(4.6)	75.1(3.2)	76.0	79.3(10.3)	79.2(10.2)	
$CH_3NH_3^+$	59.4(2.3)	59.4(1.2)	71.0	60.9(3.9)	60.9(3.9)	

TABLE IV: The experimental[45,68] hydration energies and the electrostatic and nonelectrostatic contributions (in parenthesis) to the total excess chemical potential,and the enthalpies for hydrated polyatomic ions (kcal/mol), calculated by the PLHNC+RBC and the HNC+RBC models.

demonstrate the correlations between the computed and the experimental hydration energies and enthalpies for molecular and atomic ions, respectively. Therefore, the HNC+RBC and PLHNC+RBC models are satisfactory to estimate hydration energies of molecular and atomic ions, since it provides the hydration energies for the selected ions within 5-10% of accuracy. Although our results are dependent on the force field parameters, we believe that this drawback can be eliminated by an appropriate choice of the bridge functions. A 'smart' strategy for making this choice will be a matter of our forthcoming study.

We have also studied how the improved RISM models treat the electrostatic properties of hydrated ions. Figure 3 shows the comparison of the data on the distance dependence of the electrostatic potential $\Phi(r) = 8\pi n_0 q_H \int_0^\infty [h_{BrH}(r) - h_{BrO}(r)]rdr$ of Br^- hydrated

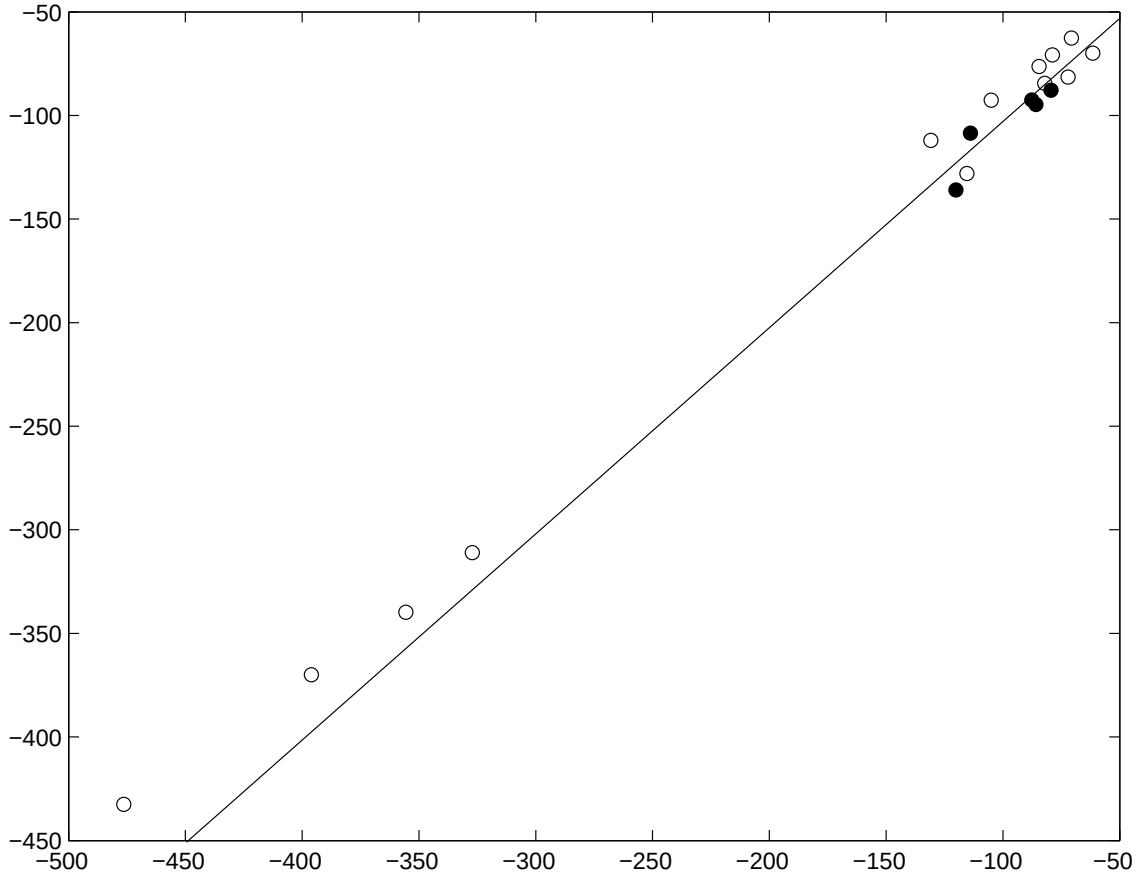

FIG. 2: The computed (RISM/HNC+RBC) versus experimental[45] hydration enthalpies for molecular and atomic ions (in kcal/mol). The notions are the same as in Fig. 1.

in water under normal conditions. Although the RDFs calculated by integral equations are different from what obtained by the MD with the use of the GROMACS package[71], the difference between the HNC+RBC and the MD data are minor[72]. In contrast to the simple HNC closure the bridge correction is able to provide accurate calculations for the electrostatic potential at small distances.

To analyze the charge effect on the electrostatic potential we have calculated the potential versus the charging parameter. The dependence of electrostatic potential on the charging parameter is close to the linear one[66], slightly deviating from the linear behaviour at small solute charges. The employment of the repulsive bridge does not change qualitatively this behaviour, although the nonlinear effects become more pronounced. Figure 4 shows the derivative of the electrostatic potential versus the charging parameters λ_{el} for NH_4^+ and

Molecule	$-T\Delta S_{el}$		$-T\Delta S_{nel}$		$-T\Delta S_{pol}$		EXP
	HNC	PLHNC	HNC	PLHNC	HNC	PLHNC	
OH^-	12.7	11.1	2.4	3.4	2.6	2.6	10.1
CN^-	3.9	3.8	3.0	4.2	0	0	4.4
OCl^-	7.2	6.9	5.6	6.6	2.7	2.7	
NH_4^+	4.8	3.7	2.0	3.0	-0.3	-0.2	6.6
$HCOO^-$	5.6	5.3	2.1	3.5	1.5	1.5	5.9
CH_3O^-	9.9	9.4	2.7	3.9	4.2	4.1	
HCC^-	7.3	7.1	3.6	4.7	2.7	2.6	
NH_2^-	11.0	10.3	3.1	4.2	3.4	3.3	
HO_2^-	10.4	9.7	2.1	3.2	2.4	2.4	
H_3O^+	4.7	4.9	1.8	2.9	1.2	1.1	8.9
CH_3COO^-	7.4	7.1	4.0	5.0	3.3	3.4	
$(CH_3)_3C^+$	0.2	-0.7	5.7	7.2	0.6	0.6	
CH_3S^-	4.1	4.1	5.7	7.1	2.4	2.4	
$CH_3NH_3^+$	1.6	1.5	1.7	2.7	0.2	0.2	

TABLE V: The experimental[45] and the calculated electrostatic (S_{el}), nonelectrostatic (S_{nel}), and the polarization (S_{pol}) contributions to the entropies of hydrated polyatomic ions (kcal/mol).

OH^- ions. As it is seen, this dependence is well approximated by the third-order polynom like as for atomic charged solutes (see for example Fig. 4 in[74]). But the approximating coefficients are quite different for anions and cations. Such behaviour clearly indicates the asymmetry of the hydration for anions and cations, however few universal classes of hydrated ions can be revealed. Such universal classes have been previously studied by MD for atomic ions[75].

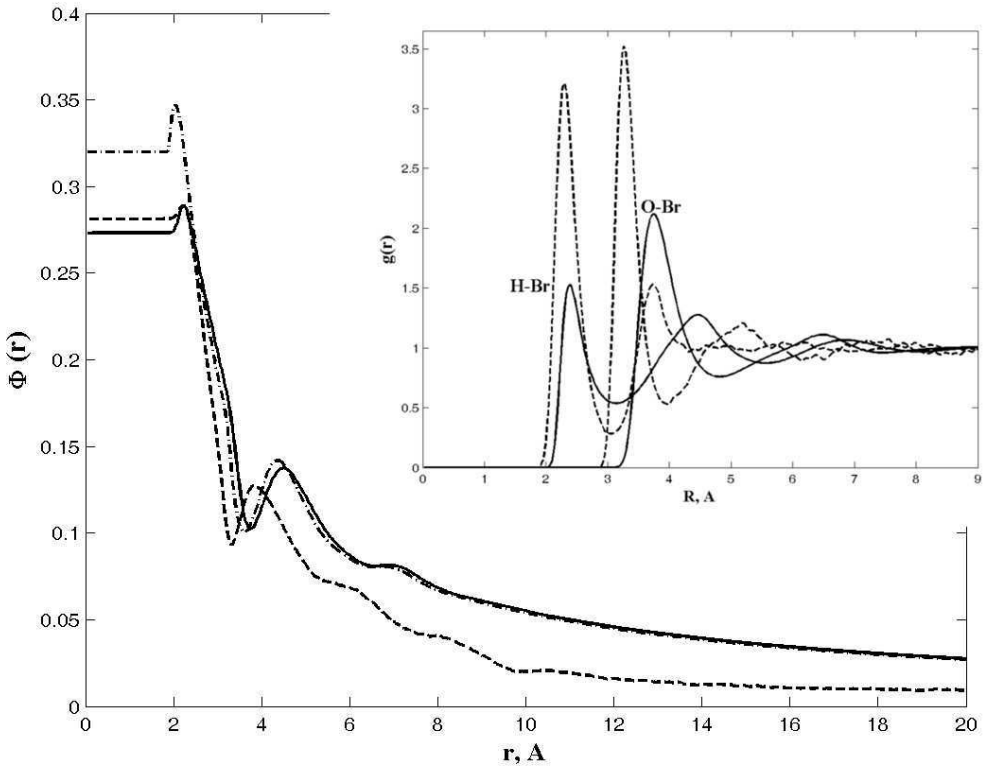

FIG. 3: The distance dependence of the electrostatic potential $\Phi(r)$ measured in atomic units for Br^- ion hydrated in water under normal conditions. The solid curve corresponds to the MD calculations, while the dashed one to the RISM/HNC+RBC, while the dotted one to the HNC evaluations. The inset shows the RDF $h_{BrH}(r) - h_{BrO}$ of Br^- hydrated in water under normal conditions.

We have also compared the accuracy of the computation of electrostatic potential. Figure 5 demonstrates the correlation between calculations of absolute values of the electrostatic potential at atoms of molecular ions. The QM calculations are provided by the PCM, the RISM data by the HNC+RBC model. As it is seen, the calculations by the improved HNC model is quite satisfactory with respect to that obtained by the QM methods.

Thus, using the 1D RISM/HNC+RBC and the 1D RISM/PLHNC+RBC models we evaluated systematically the structural and thermodynamic properties for series of hydrated atomic and molecular ions. We have shown that the above models are able to satisfactory predict the hydration energies as well as the electrostatic potential around the charged

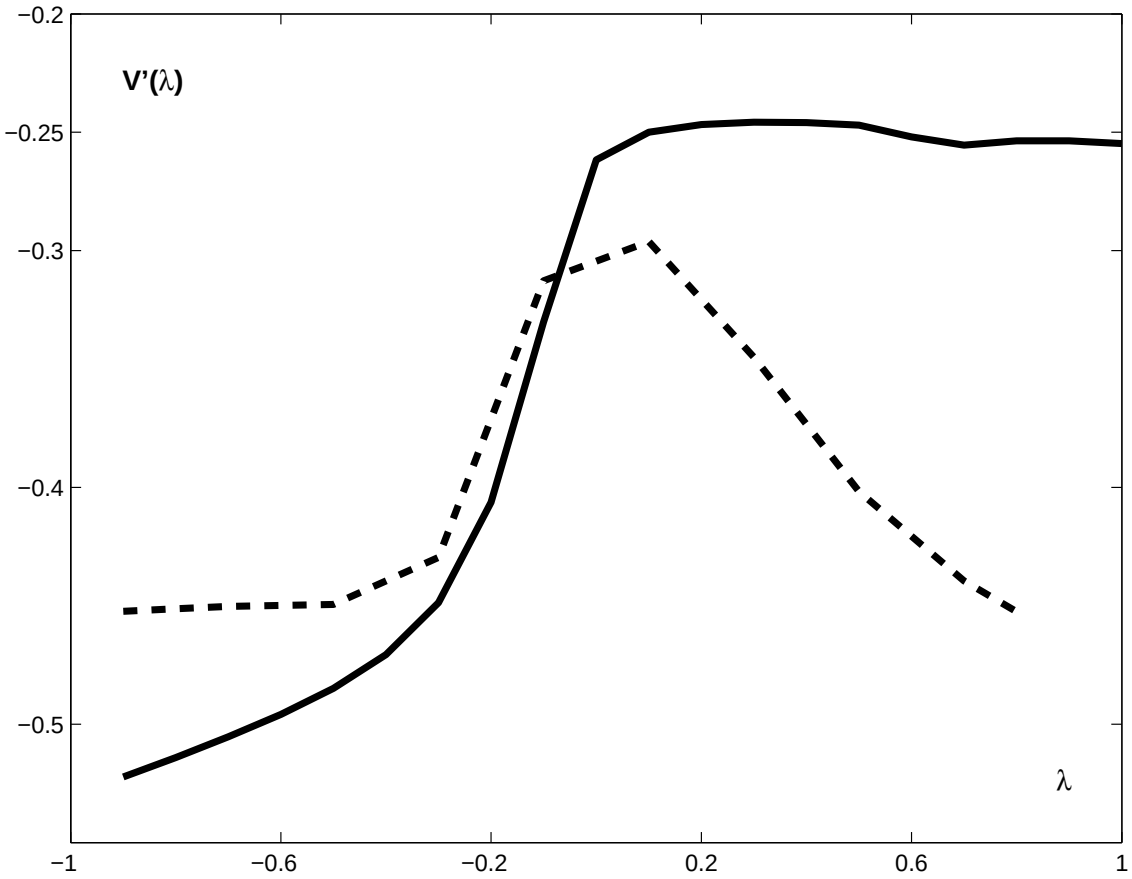

FIG. 4: The derivative $V'_u = \partial V_u/\partial\lambda$ of the electrostatic potential with respect to the charge versus charging parameters λ_{el} solid line corresponds to nitrogen in NH_4^+, while the dashed one to oxygen in OH^-.

solutes. For univalent atomic ions they provide qualitative estimates of the Samoilov activation energy. Although the evaluations of nonelectrostatic entropic contributions are not in agreement with the experimental data, we believe that this drawback can be eliminated by an additional parameterization of the repulsive bridge similar to that has been done in Ref.[28].

The advantage of the models is that they operate only with the radial distributions of the solvent atoms around solute sites and, therefore, are essentially simpler and faster than the 3D RISM treatment. Within the framework of the models we have to evaluate only $\Delta\mu_{nel}$, $V_u(0)$, and V'_{su} for computing the solvation free energy of ions. This can be done before quantum computations and then stored. More sophisticated analysis of the accuracy of different hybrid RISM-QM methods will be presented in the forthcoming paper.

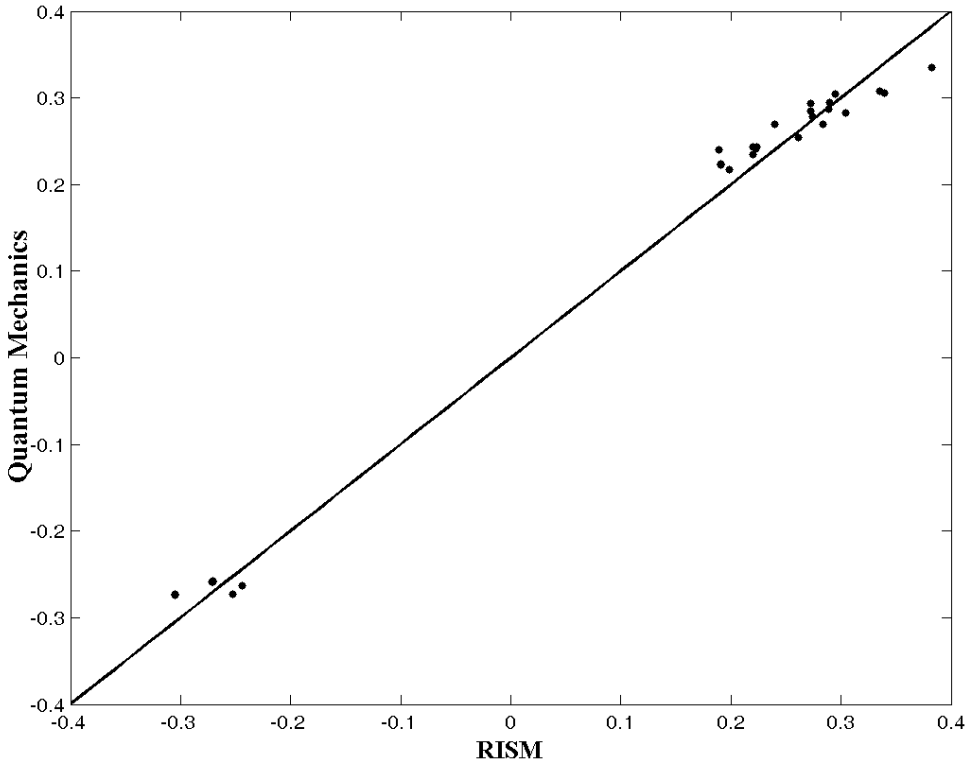

FIG. 5: The correlation between the calculations of absolute values of the electrostatic potential at atoms of molecular ions. The QM calculations are provided by the PCM, the RISM data by the HNC+RBC models.

Acknowledgments. This work was supported partially by the Russian Foundation of Basic Research.

---

[1] Gurney, R. W. Ionic Processes in Solution; McGraw Hill: New York, 1953.

[2] Samoilov, O. Y. Structure of Aqueous Electrolyte Solutions and the Hydration of Ions; Consultants Bureau, Enterpr. Inc.: New York, 1965.

[3] Franks, F. Water, a Comprehensive Treatise: Plenum: New York, 1973, Vol. III.

[4] Pratt, L. R.; Hummer, G. Simulation of Electrostatic Interactions in Solution; AIP: New York, 1999.

[5] Born, M. Z Phys 1920, 1, 45.

[6] Brooks, C. L., III; Karplus, M.; Pettitt, B. M. In Advances in Chemical Physics; Prigogine, I., Rice, S. A., Eds.; John Wiley & Sons: New York, 1988; Vol. LXXI.

[7] Allen, M. P.; Tildesley, D. J. Computer Simulation of Liquids; Oxford Science Publications: Clarendon Press: Oxford, 1989.

[8] Chandler, D.; Andersen, H. C. J Chem Phys 1972, 57, 1930-1937.

[9] Blum, L.; Torruella, A. J. J Chem Phys 1972, 56, 303-310.

[10] Fries, P. H. ; Kunz, W.; Calmettes, P. ; Turq, P. J Chem Phys 1994, 101, 554-577.

[11] Richardi, J.; Fries, P. H.; Fischer, R.; Rast, S.; Krienke, H. J Mol Liq 1997, 73-74, 465-485.

[12] Richardi, J.; Fries, P. H.; Krienke, H. J Chem Phys 1998, 108, 4079-4089.

[13] Richardi, J.; Fries, P. H.; Fischer, R.; Rast, S.; Krienke, H. Mol Phys 1998, 93, 925-938.

[14] Richardi, J.; Millot, C.; Fries, P. H. J Chem Phys 1999, 110, 1138-1147.

[15] Hansen J. P.; McDonald, I. R. Theory of Simple Liquids; Academic: London, 1976.

[16] Monson, P. A.; Morriss, G. P. Adv Chem Phys 1990, 77, 451-550.

[17] Hirata, F.; Rossky, P. J. Chem Phys Lett 1981, 83, 329-334.

[18] Hirata, F.; Pettit, B. M.; Rossky, P. J. J Chem Phys 1982, 77, 509-520.

[19] Hirata, F. Bull Chem Soc Jpn 1998, 71, 1483-1499.

[20] Beglov, D.; Roux, B. J Chem Phys 1995, 103, 360-364.

[21] Beglov, D.; Roux, B. J Phys Chem B 1997, 101, 7821-7826.

[22] Cortis, C. M.; Rossky, P. J.; Friesner, R. A. J Chem Phys 1997, 107, 6400-6414.

[23] Kawata, M.; Cortis, C. M.; Friesner, R. A. J Chem Phys 1998, 108, 4426-4438.

[24] Kovalenko, A.; Hirata, F. Chem Phys Lett 1998, 290, 237-244.

[25] Kovalenko, A.; Ten-no, S; Hirata, F. J Comput Chem. 1999, 20, 928-936.

[26] Kovalenko, A.; Hirata, F. J Chem Phys 1999, 110, 10095-10112.

[27] Kovalenko, A.; Hirata, F. J Phys Chem B 1999, 103, 7942-7957.

[28] Du, Q.; Beglov, D.; Roux, B. J Phys Chem B 2000, 104, 796-805.

[29] Kovalenko, A.; Hirata, F. J Chem Phys 2000, 113, 2793-2805.

[30] Kovalenko, A.; Truong, T. N. J Chem Phys 2000, 113, 7458-7470.

[31] Kovalenko, A.; Hirata, F. J Chem Phys 2000, 112, 10391-10402.

[32] Kinoshita, M.; Hirata, F. J Chem Phys 1996, 104, 8807-8815.

[33] Kovalenko, A.; Hirata, F.; Kinoshita, M. J Chem Phys 2000, 113, 9830- 9836.

[34] Yokogawa, D.; Sato, H.; Sakaki, S. J Chem Phys 2005, 123, 211102 1-5.

[35] Yokogawa, D.; Sato, H.; Sakaki, S. Chem Phys Lett 2006, 432, 595599.

[36] Gao, J. Acc Chem Res 1996, 29, 298-305.

[37] Ten-no, S.; Hirata, F.; Kato, S. Chem Phys Lett 1993, 214, 391- 396.

[38] Ten-no, S.; Hirata, F.; Kato, S. J Chem Phys 1994, 100, 7443- 7453.

[39] Sato, H.; Hirata, F.; Kato, S. J Chem Phys 1996, 105, 1546- 1551.

[40] Sato, H.; Kovalenko, A.; Hirata, F. J Chem Phys 2000, 112, 9463-9468.

[41] Gusarov, S.; Ziegler, T.; Kovalenko A. J Phys Chem A 2006, 110, 6083-6090.

[42] Yokogawa, D.; Sato, H.; Sakaki, S. J Chem Phys 2007, 126, 244504 1- 6.

[43] Yokogawa, D.; Sato, H.; Sakaki, S. J Mol Liq 2007, 136, 190- 193.

[44] Samoilov, O. Y. Discuss Faraday Soc 1957, 24, 141- 146.

[45] Florian, J.; Warshel, A. J Phys Chem B 1997, 101, 5583-5595.

[46] Singer, S.J.; Chandler, D. Mol Phys 1985, 55, 621-625.

[47] Kirkwood, J. G. J Chem Phys 1935, 3, 300-313.

[48] Hummer, G.; Pratt, L. R.; Garcia, A. E. J Phys Chem 1996, 100, 1206-1215.

[49] Fedorov, M. V.; Kornyshev, A. A. Mol Phys 2007, 105, 1-16.

[50] Du, Q.; Wei, D. J Phys Chem B 2003, 107, 13463-13470.

[51] Kovalenko, A.; Hirata, F.; Kinoshita, M. J Chem Phys 2000, 113, 9830-9836.

[52] Jorgensen, W. L. ; Maxwell, D. S.; Tirado-Rives, J. J Am Chem Soc 1996, 117, 11225-11236.

[53] Jorgensen, W. L.; Ulmschneider, J. P.; Tirado-Rives, J. J Phys Chem B 2004, 108, 16264-16270.

[54] Besler, B. H.; Merz, K. M.; Kollman, P. A. J Comput Chem 1990, 11, 431-439.

[55] Köster, A. M.; Geudtner, G.; Goursot, A.; Heine, T.; Vela, A.; Salahub, D. R. deMon2001; NRC: Ottawa, 2001.

[56] Vosko, S. H.; Wilk, L.; Nusair, M. Can J Phys 1980, 58, 1200-1211.

[57] Sato, H.; Sakaki, S. J Phys Chem A 2004, 108, 1629-1634.

[58] Godbout, N.; Salahub, D. R.; Andzelm, J.; Wimmer, E. Can J Chem 1992, 70, 560-571.

[59] Lue L.; Blankschtein, D. J Phys Chem 1992, 96, 8582-8594.

[60] Cummings, P. J.; Stell, G. Mol Phys 1981, 44, 529.

[61] Rossky, P. J.; Pettitt, B. M.; Stell, G. Mol Phys 1983, 50, 1263.

[62] Raineri, F. O.; Stell, G. J Phys Chem B 2001, 105, 11880-11892.

[63] Chuev, G. N.; Fedorov, M. V. J Comput Chem 2004, 25, 1369-1377.

[64] Chuev, G. N.; Fedorov, M. V. J Chem Phys, 2004, 120, 1191-1196.

[65] Fedorov, M. V.; Flad, H-J.; Chuev, G. N.; Grasedyck, L., Khoromskij, B. N. Computing 2007 80, 47-73.

[66] Chuev, G. N.; Chiodo, S.; Erofeeva, S. E.; Fedorov, M. V.; Russo, N.; Sicilia, E. Chem Phys Lett 2006, 418, 485-489.

[67] Chiodo, S.; Chuev, G. N.; Erofeeva, S. E.; Fedorov, M. V.; Russo, N.; Sicilia, E. Int J Quantum Chem, 2006, 107, 265-274.

[68] Pliego, J. R. Jr.; Riveros, J. M. Phys Chem Chem Phys. 2002, 4, 1622-1627.

[69] Chong, S. H.; Hirata, F. J Phys Chem B 1997, 101, 3209-3220.

[70] Fedorov, M. V.; Goodman, J. M.; Schumm, S. Phys Chem Chem Phys 2007, 9, 5423-5435.

[71] van der Spoel, D.; Lindahl, E.; Hess, B.; Groenhof,G.; Mark A. E.; Berendsen, H. J. C. J Comput Chem 2005, 26, 1701-1718.

[72] We have used the geometric rule for solute-solvent diameter σ_{uj}, to compare the results with the MD data obtained by GROMACS with the OPLS force field.

[73] Chuev G. N.; Fedorov M. V.; Crain J. Chem Phys Lett 2007, 448 198202.

[74] Hummer, G.; Pratt, L. R.; Garcia, A. E. J Am Chem Soc 1997, 119, 8523-8527.

[75] Lynden-Bell, R. M.; Rasaiah, J. C. J Chem Phys 1997, 107, 1981-1991.